International Journal of Precision Engineering and Manufacturing-Green Technology (2023) 10:35–44
https://doi.org/10.1007/s40684-022-00416-0

Online ISSN 2198-0810
Print ISSN 2288-6206

REGULAR PAPER

Study on Cutting Force and Tool Wear in Machining of Die Materials with Textured PCD Tools Under Ultrasonic Elliptical Vibration

Sangjin Maeng[1] · Hiroaki Ito[2] · Yasuhiro Kakinuma[2] · Sangkee Min[3]

Received: 14 July 2021 / Revised: 16 October 2021 / Accepted: 4 January 2022 / Published online: 1 February 2022

Abstract
Machining of steel-based alloy (STAVAX) and tungsten carbide (WC) is very challenging due to their superior hardness. Severe wear in the machining of the die materials is the dominant problem. Texturing on the rake face of the tool and ultrasonic elliptical vibration cutting (UEVC) may resolve this issue and could prolong tool life. The patterns on the rake face of the tool entrap the chip and debris created in machining and prevent abrasion. During UEVC the flank face of the tool does not contact the workpiece and the rake face of the tool helps the chip evacuate from the machining area when the tool disengages with the workpiece. Thus, UEVC reduces cutting force and tool wear compared to conventional cutting. This paper investigates the cutting performance and tool wear in machining of the die materials with textured polycrystalline diamond (PCD) tools under UEVC. The linear patterns parallel or perpendicular to the chip flow are engraved on the rake face of the PCD tools with the focus ion beam (FIB) process. Orthogonal cutting experiments are carried out on ultra-precision machine tools with and without UEVC. Machining under UEVC remarkably reduces the cutting and thrust force and improves tool life. For machining of STAVAX with the textured PCD tool, the linear patterns alone do not improve the cutting, but they improve the cutting when they are combined with UEVC. In machining of WC, the linear pattern becomes effective by slightly decreasing the thrust force and friction coefficient when UEVC is not applied.

Keywords Machinability · Friction · Ultrasonic elliptical vibration cutting

1 Introduction

STAVAX as a steel-based alloy and tungsten carbide (WC) are widely used in the die and mold industry due to their superior strength and thermal stability [1, 2]. One of the possible tools for machining these hard materials is a polycrystalline diamond (PCD) tool which is stronger than those materials. As the high cutting force is subjected to the tool surface during machining of the hard materials with the PCD tool, the tool is quickly worn out due to abrasive wear. The high force also introduces more heat, thereby increase of the temperature shortens the tool life [3].

Texturing on the rake face of the tool is one of the available technologies to reduce the friction force on the rake face between a tool and workpiece. The pattern on the rake face of the tool entraps the chips and debris generated in machining and prevents abrasion on the rake face of the tool. Many researchers have evaluated the effectiveness of the patterns on reduction of the cutting force in the machining process. Hao et al. fabricated a PCD tool with linear patterns with composite lyophilic/lyophobic wettability by a pulsed fiber laser. They observed that the friction coefficient decreased by about 11% and the tool life was improved since chip adhesion on the tool surface was alleviated in the machining of Ti-6Al-4 V with the patterned tool [4]. Kim et al. machined bearing steel with the cubic boron nitride (CBN) tool with micro-textures. After applying the textured CBN tool, the friction coefficient decreased by 28% than a non-patterned tool [5]. Kawasegi

✉ Yasuhiro Kakinuma
kakinuma@sd.keio.ac.jp

✉ Sangkee Min
sangkee.min@wisc.edu

[1] Department of Mechanical and System Design Engineering, Hongik University, 94 Wausan-ro, Mapo-gu, Seoul 04066, Republic of Korea

[2] Department of System Design Engineering, Faculty of Science and Technology, Keio University, 3-14-1 Hiyoshi, Kohoku-ku, Yokohama, Japan

[3] Department of Mechanical Engineering, University of Wisconsin-Madison, 1513 University Ave, Madison, WI 53706, USA

et al. created a single crystalline diamond (SCD) tool with linear patterns on the rake face using a focused ion beam (FIB) process followed by heat treatment and machined aluminum and nickel-phosphorus alloys. The cutting with the SCD tool with linear patterns perpendicular to the chip flow direction reduced the friction coefficient by about 18% [6]. Kang et al. fabricated carbide tools with concave and convex microtextures and found the effectiveness of the patterns on the reduction of friction force and normal force by 15% and 10%, respectively [7]. Lian et al. also fabricated the microtextures on the rake face of the cemented carbide tool. In machining of AISI 1045 carbon steel, they revealed reduction of the cutting force, cutting temperature, and friction coefficient and highlighted the anti-adhesive property of the textured tool [8]. Zhang et al. also reported that the microtextures had an advantage in reduction of anti-adhesive force between the rake face of the tool and the chips in machining of AISI 316L stainless steel [9]. In previous work, WC workpiece was machined with a PCD tool with linear patterns parallel and perpendicular to the chip flowing direction and the most improvement in reduction of friction coefficient was 10% [10]. The previous studies have fabricated various shapes of patterns on WC, CBN, PCD, and SCD tools and evaluated the tool performance on aluminum, carbon steel, stainless steel, titanium alloy, and nickel alloy in terms of cutting force.

Another method to reduce the cutting force and tool wear is ultrasonic elliptical vibration cutting (UEVC). Shamoto et al. proposed the UEVC first in 1994 [11]. The technology was successfully applied for cutting hardened steel, nickel alloy, tungsten carbide, and ceramics. Shamoto and Moriwaki machined hardened steel with UEVC and showed significant improvement in surface quality and tool life and reduction in cutting force [12]. Kim et al. machined pure nickel, nickel alloy, and mold steels with SCD and CBN tool under UEV. The machining quality was improved and the production time was significantly reduced [13]. Liu et al. reported the increase of the critical uncut chip thickness which was the transition from the ductile to brittle cutting mode in machining of tungsten carbide after applying the vibration-assisted cutting [14]. Suzuki et al. also found that the critical uncut chip thickness for the ductile cutting mode was significantly increased in machining of an optical glass part under UEVC [15]. During UEVC the flank face of the tool does not contact the machined surface of the workpiece when the tool disengages with the workpiece. As the tool moves out in chip flow direction, the rake face of the tool helps the chip evacuate from the machining area. Compared to conventional cutting, UEVC reduces cutting force and tool wear [16]. Therefore, UEVC is widely used for turning, milling, drilling, and grinding processes as well as fabricating micro patterns, features, and textures, efficiently [17–19].

This study investigates the synergistic effect of patterned tools with ultrasonic elliptical vibration (UEV) on STAVAX and WC. The linear patterns parallel and perpendicular to the chip flow are engraved with the FIB process and their cutting performances were compared with non-patterned tools and application of UEV.

2 Textured PCD Tool

Linear patterns parallel and perpendicular to the chip flowing direction were fabricated on the rake face of the PCD tool (DA1000, Sumitomo tool, Japan) with FIB process as shown in Fig. 1a, b. The PCD tool has less than 0.5 μm in grain size and 110–120 GPa in Hv hardness which is much harder than STAVAX and WC. The FIB machining conditions were 30 kV acceleration voltage, 3.0 nA beam size, and gallium ion. 60 parallel lines were engraved with a width of 1 μm, a depth of 1 μm, and a pitch of 2 μm. Each line starts at about 2 μm from the cutting edge and ends at 9 μm from the highest point of the cutting edge. The perpendicular patterns have 4 lines with width of 1 μm, depth of 1 μm, pitch of 2 μm, and length varied along with the tool nose. The length of the lines is from 50 to 120 μm and the shortest line starts at about 2 μm from the cutting edge. The engraved areas of the parallel and perpendicular patterns on the rake face are equal. The pattern length in the cutting direction should be equal to or less than the tool-chip contact length.

3 Ultrasonic Elliptical Vibration Cutting (UEVC)

Ultrasonic elliptical vibration cutting causes the tool to move in a small circle or ellipse as shown in Fig. 2. The periodic movement in ultrasound frequency along the workpiece

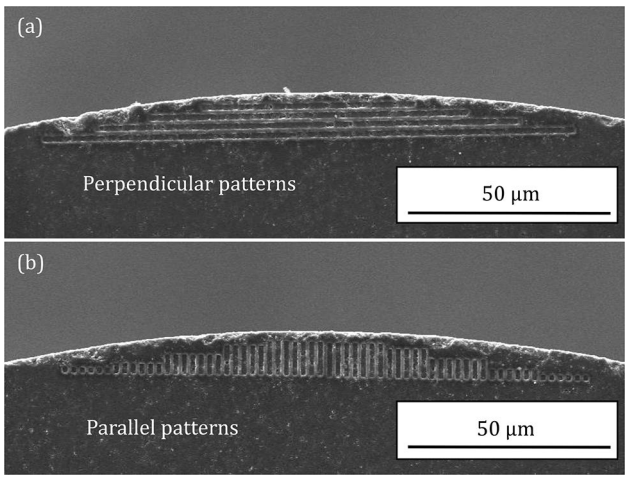

Fig. 1 SEM image of the linear patterns (**a**) perpendicular and (**b**) parallel to the chip flowing direction

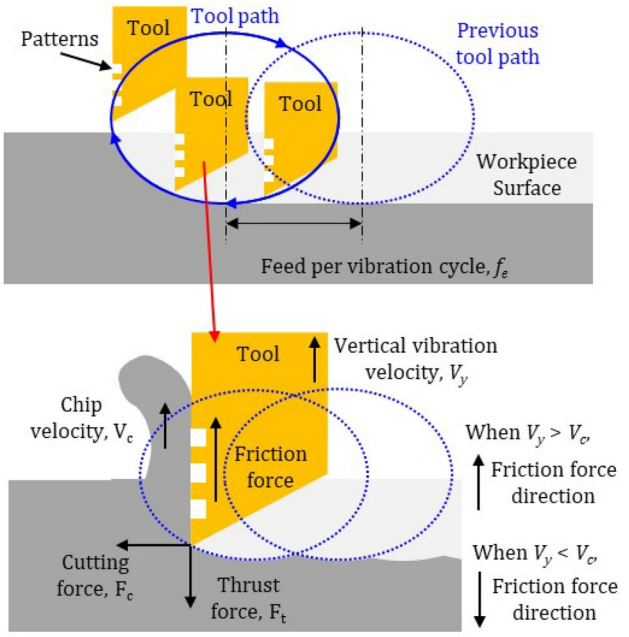

Fig. 2 Schematic of UEVC; When the vertical vibration velocity is faster than the chip velocity, the friction force pulls off the chip

surface leads to lose the contact with the chip and the workpiece. As a result, the cutting force is significantly reduced, and the chip become thinner [16]. In machining of ferrous materials with a diamond tool, the reduced contact time also reduces the diffusion wear [20]. The tool trajectory can be derived as follow:

$$x(t) = A\cos(\omega t) + Vt \tag{1}$$

$$y(t) = B\sin(\omega t) \tag{2}$$

Velocity of the tool can be calculated from Eq. (1) and (2):

$$V_x(t) = -A\omega\sin(\omega t) + V \tag{3}$$

$$V_y(t) = B\omega\cos(\omega t) \tag{4}$$

where V, ω, A, and B are cutting speed, angular frequency, and horizontal and vertical amplitude of the vibration, respectively. To achieve the benefit of interrupted cutting under UEVC, the maximum speed in horizontal direction, $A\omega$ must be larger than cutting speed, V and the amplitude in vertical direction, B must be larger than the depth of cut. In the experiment, the vibration frequency of 40 kHz and the maximum amplitude of 4 μm were used with the UEVC device (EL-50, Tagadennki, Japan). As the horizontal vibration speed is 64 times faster than the cutting speed, 150 mm/min and the amplitude in the vertical direction is higher than the depth of cut, the cutting mode under UEVC in the experiment was interrupted cutting.

Table 1 Material properties of STAVAX and WC

Properties	STAVAX	WC
Hardness	33 HRC	77 HRC
Young's modulus, E	200 GPa	523 GPa
Tensile strength	1130 MPa	2270 MPa
Composition	Fe (> 85%), Cr (> 13%), C, Mn, Si, V (< 1%),	W (> 90%), Co (7.5%)

In conventional machining, the chip flows along the rake face of the tool and the friction occur at the interface between the chip and rake face. The direction of friction force is opposite to the chip flow and hinders from evacuating chips from the machined area. The vertical vibration reduces the friction force or changes the direction reversely and affects the chip flow. When the vertical velocity of the tool is much faster than the chip flow, the direction of the friction is reversed, and the friction force help to pull up the chip from the machined area. The reversed friction force significantly reduces the cutting force and heat generation [11]. Here, the patterns on the rake face of the tool would influence the friction coefficient and help to pull away the chip effectively. In machining of ductile materials, the patterns may pull off the continuous chip more effectively than brittle materials because the chip of brittle material is easily broken and the chip cannot escape along with the tool by friction force.

4 Experiments

Orthogonal cutting experiments on STAVAX and WC workpiece, Table 1, with UEV were carried out on UVM-450C (Shibaura machine, Japan), and cutting experiments without UEV were conducted on ROBONANO α-0*i*B (FANUC Corporation, Japan) as shown in Fig. 3. Specifications of the machine tools are listed in Table 2. Note that preliminary cutting experiments were conducted in order to verify the difference between the two machine tools' performance since the cutting experiments were done with two ultra-precision machine tools. Al6061 was machined for a varied depth of cut on two machine tools and the difference of the cutting and thrust force between the two machines were within 5% at the same depth of cut. The workpiece was installed on a dynamometer (9119AA1, Kistler) which measures the cutting force in x-, y-, and z-axis simultaneously. The sampling rate of the measured cutting force was 40 kHz. As the cutting force is

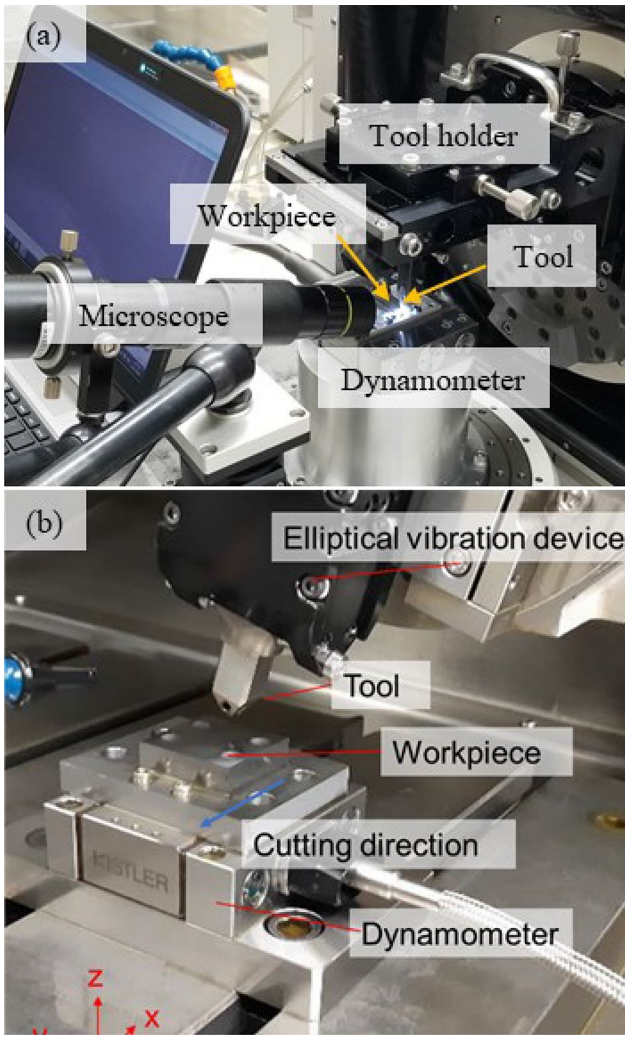

Fig. 3 Experiment setup in (**a**) ROBONANO α-0*i*B and (**b**) UVM-450C with the UEV device

Table 2 Specification of the machine tools

Specification	ROBONANO α-0*i*B	UVM-450C
Programming resolution [nm]	1	10
Axes	X, Y, Z, B, and C	X, Y, Z, A, and C
Max. feedrate [m/min]	X and Z: 0.5, Y 0.05	X and Y: 15, Z 10
CNC system	FANUC Series 30*i* Model B	
Bearing type	Aerostatic bearing	

fluctuating, the average of 500 samples of the cutting force and thrust force was calculated.

Orthogonal cutting experiments for short and long distance were conducted under lubricant to evaluate the reduction of cutting force and the tool wear, respectively. In short distance experiments, Fig. 4, the orthogonal cutting was performed for 5 mm with varying depth of cut from 0.5 to 5 µm. In long distance machining, the depth of cut and width of cut were fixed as 1 µm and the machining length was 5 m. Note that the machining distance for long distance machining of WC without UEV was only 1 m because the thrust force rapidly increased and the machine tool was overloaded after 1 m in machining distance. Rake angle and feedrate were fixed as 0° and 150 mm/min, respectively.

5 Results and discussion

Figures 5 and 6 show cutting force, thrust force, and friction coefficient for the actual depth of cut (DOC) for short distance cutting of STAVAX and WC, respectively. Here, the friction coefficient was calculated from thrust force and cutting force follow:

$$\mu = \frac{F}{N} = \frac{F_c sin\alpha + F_t cos\alpha}{F_c cos\alpha - F_t sin\alpha} \tag{5}$$

where Fc, Ft, and α are cutting force, thrust force and rake angle, respectively. As the rake angle was fixed as 0°, the friction coefficient is the thrust force over cutting force. The actual DOC which was defined as the distance between the lowest point and the surface adjacent to the machined area was measured with a white light interferometer. The cutting force and thrust force are proportional to the actual DOC, while the friction coefficient decreases as the actual DOC increases. Since the edge radius of the PCD tool is about 2 µm, the thrust force is larger than the cutting force at the actual DOC lower than the edge radius and gradually becomes smaller than the cutting force as the actual DOC increases. Hence, the friction coefficient is inversely proportional to the actual DOC regardless of the patterns and UEV. This trend is also observed in machining of WC in Fig. 6c.

As UEVC effectively reduces the friction force between the tool and the workpiece compared to the conventional cutting, the cutting and thrust force are significantly decreased by about 93% for STAVAX and 53% for WC while patterns contribute to minor reduction of forces as shown in Figs. 5a,

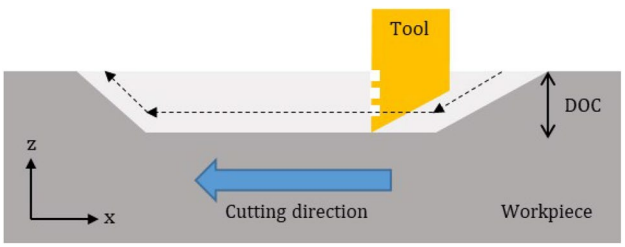

Fig. 4 Schematic of orthogonal cutting for short distance

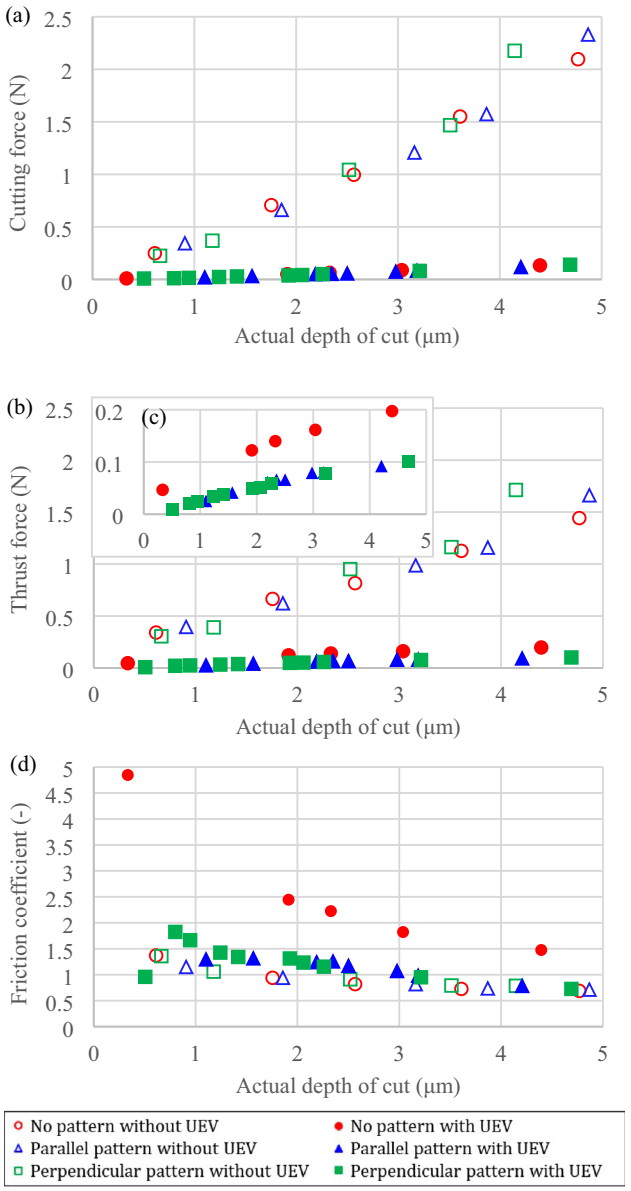

Fig. 5 **a** Cutting force, **b** thrust force, **c** thrust force under UEV zoomed in from 0 to 0.2 N, and **d** friction coefficient in machining of STAVAX for actual depth of cut in 5 mm distance cutting

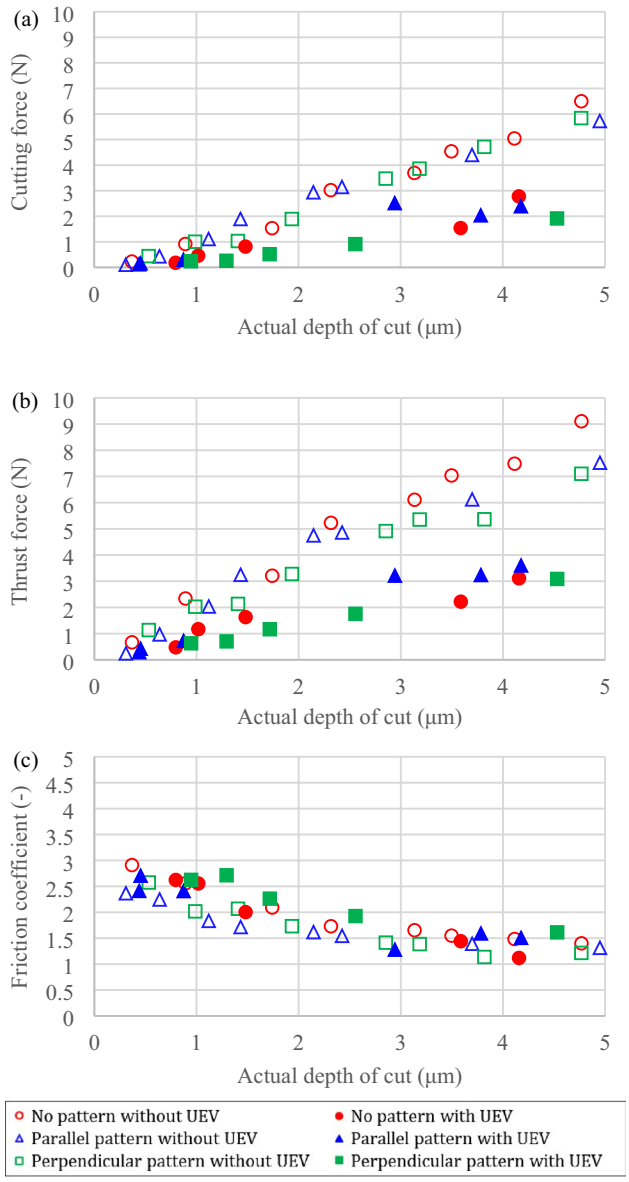

Fig. 6 **a** Cutting force, **b** thrust force, and **c** friction coefficient in machining of WC for actual depth of cut in 5 mm distance cutting

b and 6a, b. The result indicates that UEVC is more effective to reduce the cutting and thrust force in machining of STAVAX than WC. The difference between STAVAX and WC is ductility and chemical affinity with PCD tools. As the STAVAX chip is more adhesive to the tool, intermittent contact by UEVC dramatically decreases the cutting and thrust force. On the other hand, the WC is brittle and the chips are segmented in few micrometers in Fig. 7 so that the effect of UEVC is less than STAVAX.

The linear patterns on the rake face of the tool show an improved effect with UEV in machining of STAVAX. Thrust forces with and without the pattern are about the same when UEV is not applied, while the thrust force with the pattern is about 50% smaller than the one without the pattern under UEV, Fig. 5b, c. It implies that the patterns may act as an anchor to pull up the chip and thereby the thrust force is effectively decreased. It is noted that the friction coefficients under UEV are larger than the ones without UEV. Shamoto and Moriwaki [11] explained this phenomenon as the direction of friction is reversed in UEV and the actual shear angle becomes more than 45° degree. On the other hand, the patterns without UEV do not have the benefit to reduce friction.

In machining of WC, the linear patterns without UEV reduce the friction coefficient unlike the case with STAVAX. Figure 6b shows the thrust force in machining with

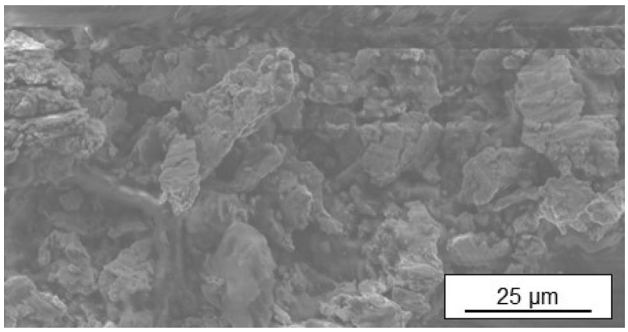

Fig. 7 SEM image of segmented WC chips

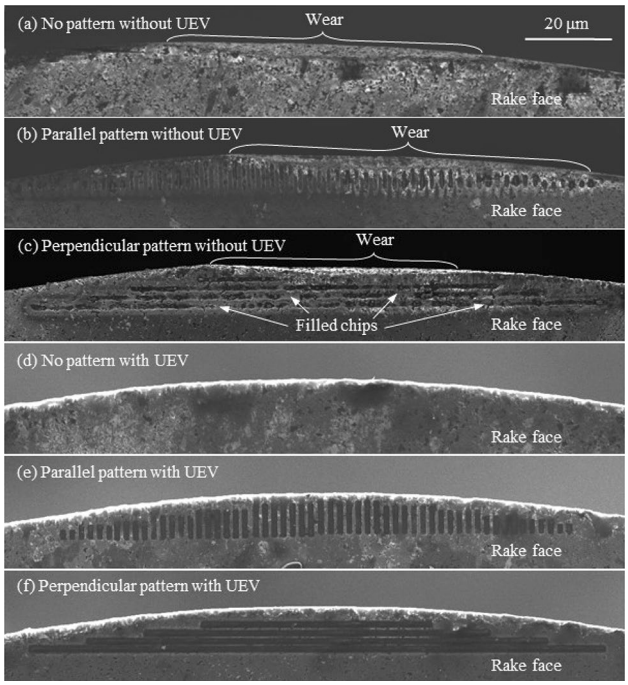

Fig. 8 SEM images of tool wear on rake face after machining of STAVAX for 5 m: **a** no pattern without UEV, **b** parallel pattern without UEV, **c** perpendicular pattern without UEV, **d** no pattern with UEV, **e** parallel pattern with UEV, and **f** perpendicular pattern with UEV

patterned tools decreases by about 15% than non-textured tools when UEV is not applied, while the patterns under UEV do not show a benefit of reducing the thrust force as the dominant effect is achieved by UEV. As the WC chip is easily segmented and less adhesive to the tool, UEV shakes off the chips from the cutting interface and the pattern is not likely to provide additional benefits. Summarizing the short distance cutting experiments, applying UEV effectively reduces the cutting and thrust force regardless of the work material. In machining of STAVAX, the linear patterns have the benefit to reduce the friction coefficient only under the UEV. The effect of the patterns under UEV in machining of WC is marginal but the thrust force and friction coefficient with the patterned tools are slightly reduced when UEV is not applied.

Tool wear progress is observed via the experiments for long distance machining of STAVAX. The edge of the PCD tool was measured with SEM after the long distance machining as shown in Fig. 8. The wear at the tool edge used in machining of STAVAX without UEV is clearly shown in Fig. 8a, b, c, while the tool wear is not detected under UEV in Fig. 8d, e, f. Dominant tool wear process in diamond tool is the disruption of the carbon–carbon bonds in the tool surface [20]. The machining under UEV reduces the contact between the PCD tool and ferrous workpiece and the tool wear on the rake face is insignificant than the machining without UEV. As the contact time between the tool and the workpiece decreases and the tool is more exposed to the lubricant, the intermittent cutting prevents from increasing the chemical activity between the PCD tool and STAVAX workpiece and increasing the temperature of the tool. Comparing, Figs. 8b, c, e, f, it is observed that the chip is more filled in the pattern without UEV. The result implies that the chip is more likely to adheres the tool surface in the continuous cutting mode and induces the adhesive wear when the chip detached from the tool surface. Therefore, the UEVC would reduce the thermal softening of the tool and the diffusion and adhesive wear on the edge and rake face of the tool.

Without UEV, the cutting and thrust force rapidly increases at the cutting length from 0 to 2 m and slowly increases from 2 cutting length to 5 m. It can be assumed that the tool is quickly worn out from 0 to 2 m distance and is stabilized afterward. An interesting observation in Fig. 9b is that the thrust force in machining with the non-textured tool is higher than the patterned tools at initial but smaller over 2 m in machining length when UEV is not applied. The result infers that the STAVAX chip slowly fills the channel in the linear pattern and acts as a tool surface with more chance of adhesion to the newly created chip than the diamond surface. Hence, the pattern filled with the chip would increase the friction force for long distance machining as shown in Fig. 9c.

Figure 10 shows SEM images of tool wear at the edge after machining of WC for 1 m without UEV and 5 m with UEV. Figure 11 shows the cutting force, thrust force, and friction coefficient for 1 m machining length without UEV and 5 m with UEV. As thrust force was rapidly increased over 1 m in machining distance without UEV, the experiment without UEV was only conducted by 1 m. Chipping is only found at the non-textured tool without UEV in Fig. 10a and the thrust force rapidly increases, Fig. 11b. After initial cutting at around 0.4 m, the patterned tools result in lower thrust force than the non-patterned tool when UEV is not applied. Hence, engraving the pattern on the tool would

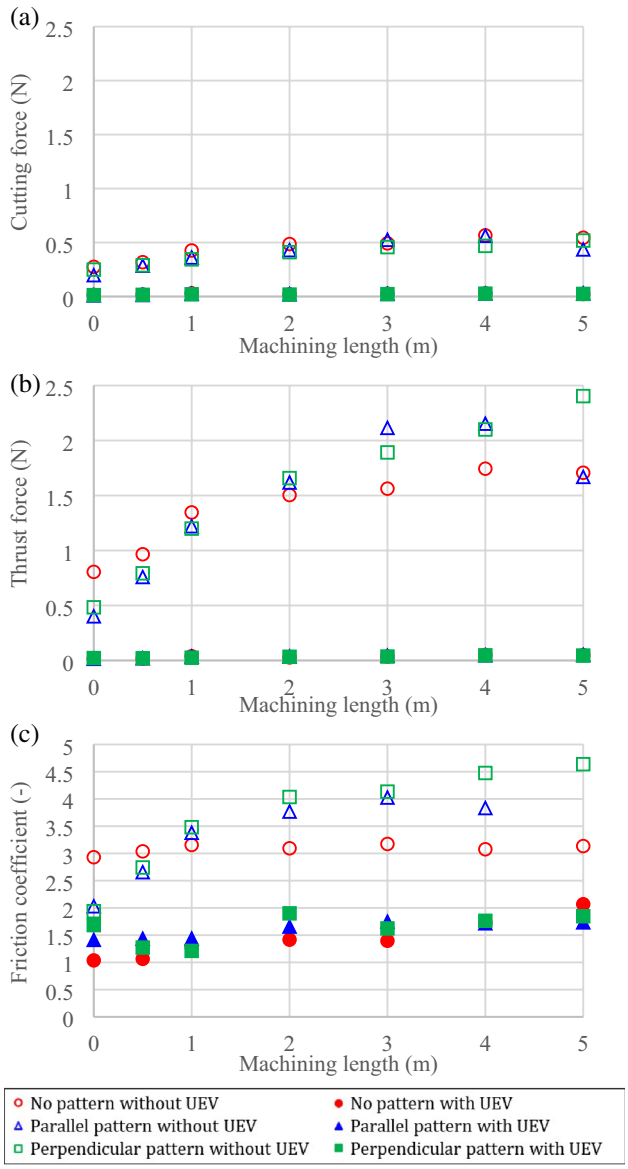

Fig. 9 **a** Cutting force, **b** thrust force, and **c** friction coefficient in machining of STAVAX for 5 m machining distance

slightly increase the tool life in machining of WC without UEV.

Under UEV, the tool wear was observed 5 m machining length as shown in Fig. 11. The cutting and thrust force with UEV are much lower than the ones without UEV regardless of the pattern in Fig. 11a, b. Comparing no pattern tool, Fig. 10a and patterned tool, Fig. 10b, c under UEV, the size of the tool wear with the no pattern tool is larger than one with patterned tools. It seems that the tool wear with pattern tool more rapidly progress than no pattern tool since the thrust force with the no pattern tool is larger than the patterned tool. Therefore, the results imply that the patterns on the tool reduce the thrust force and friction coefficient

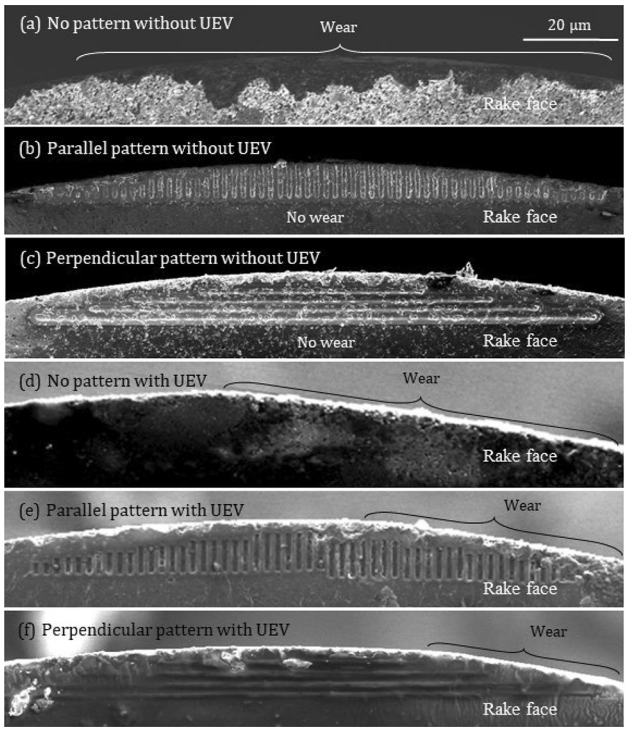

Fig. 10 SEM images of tool wear on rake face after machining of WC for 1 m: **a** no pattern without UEV, **b** parallel pattern without UEV, **c** perpendicular pattern without UEV, **d** no pattern with UEV, **e** parallel pattern with UEV, and **f** perpendicular pattern with UEV

regardless of UEV and the machining of WC can perform with lower cutting and thrust force under UEV.

Figure 12 shows the SEM image of the chip formation in machining of STAVAX. UEVC significantly reduces the chip thickness in Fig. 12. As the friction force decreases or even the direction of friction force is reversed under UEV, the shear angle become larger, and the chip thickness is thinner. Comparing Fig. 12a, c, e, the chips of non-patterned tool are thinner than the textured tools when UEV is not applied. It implies that the patterns increase friction force between the tool and the chips in machining of STAVAX. On the other hand, there was no difference in chip thickness regardless of the pattern under UEV as shown in Fig. 12b, d, f.

Figure 13 presents the chip morphology generated in machining of STAVAX with patterned tools under UEV. It is observed that the perpendicular patterns have smaller radius of curl than the parallel patterns. Interesting observation is that parallel lines are marked on the chip surface and microfibers are projected along the parallel pattern direction in Fig. 13b. This result indicates that the patterns on the rake face of the tool under UEV plastically deform the surface of the chip and may help to pull off the chip from the workpiece by the friction force effectively.

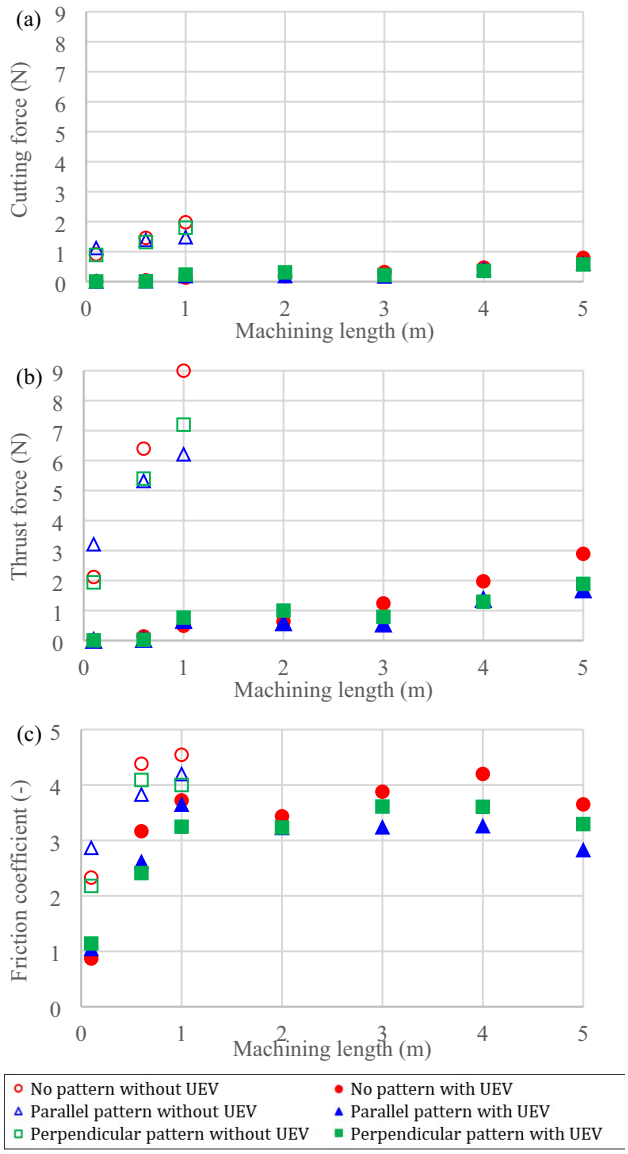

Fig. 11 **a** Cutting force, **b** thrust force, and **c** friction coefficient in machining of WC for 1 m machining distance without UEV and for 5 m machining with UEV

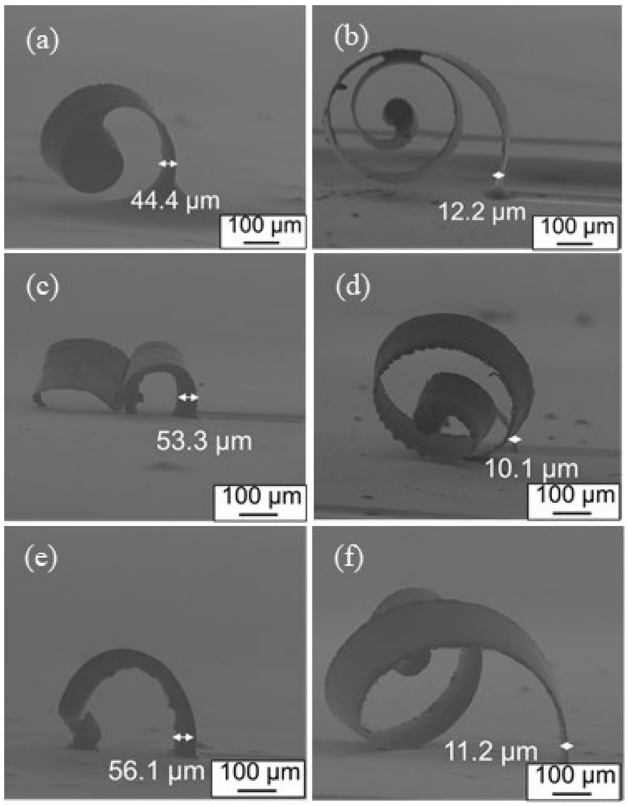

Fig. 12 Chip formation in machining of STAVAX under the conditions; (**a**) no UEV and no pattern, (**b**) UEV and no pattern, (**c**) no UEV and perpendicular pattern, (**d**) UEV and perpendicular pattern, (**e**) no UEV and parallel pattern, and (**f**) UEV and parallel pattern

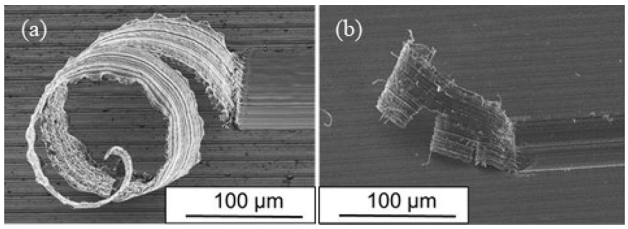

Fig. 13 Chip formation in machining of STAVAX under UEV and (**a**) perpendicular pattern and (**b**) parallel pattern

6 Conclusions

Texturing on the rake face of the tool and applying UEV are effective methods to reduce the cutting force and prolong the tool life. This study investigates the synergistic effect of the texturing and UEVC on tool wear and reduction of cutting force in machining of die steel alloy (STAVAX) and tungsten carbide (WC).

Short and long distance experiments were conducted on ultra-precision machine tools to study the effect of these methods. The following remarks are summarized as below:

- UEVC plays a dominant role in increasing tool life and remarkably reduces the cutting and thrust force in machining of both STAVAX and WC compared with the non-vibration cutting regardless of the pattern of the tool.
- For machining of steel alloy (STAVAX) with a PCD tool, the linear patterns alone do not improve the cutting, but they improve the cutting when they are combined with UEV.
- In machining of WC, the linear pattern becomes effective by slightly decreasing the thrust force and friction coefficient.

- The effect of the pattern type, parallel vs. perpendicular is marginal in all the cases.

Hence, when machining die materials, UEV is the most effective method. If further improvement for steel-based alloys is required, the pattern on the tool surface is recommended with UEV.

Acknowledgements The authors gratefully acknowledge the financial support and the donation of the ROBONANO α-0iB to MIN LAB at UW-Madison from the FANUC Corporation, Japan (MSN240845) and Sumitomo Electric Carbide, Japan for providing the diamond tools as well as the financial support from Hongik University.

References

1. Zhan, Z., He, N., Li, L., Shrestha, R., Liu, J., & Wang, S. (2015). Precision milling of tungsten carbide with micro PCD milling tool. *The International Journal of Advanced Manufacturing Technology, 77*(9), 2095–2103. https://doi.org/10.1007/s00170-014-6632-7
2. Ding, X., Liew, W. Y. H., Ngoi, B. K. A., Gan, J. G. K., & Yeo, S. H. (2002). Wear of CBN tools in ultra-precision machining of STAVAX. *Tribology Letters, 12*(1), 3–12. https://doi.org/10.1023/A:1013987708701
3. Zhao, Y., Yue, W., Lin, F., Wang, C., & Wu, Z. (2015). Friction and wear behaviors of polycrystalline diamond under vacuum conditions. *International Journal of Refractory Metals and Hard Materials, 50*, 43–52. https://doi.org/10.1016/j.ijrmhm.2014.11.008
4. Hao, X., Cui, W., Li, L., Li, H., Khan, A. M., & He, N. (2018). Cutting performance of textured polycrystalline diamond tools with composite lyophilic/lyophobic wettabilities. *Journal of Materials Processing Technology, 260*, 1–8. https://doi.org/10.1016/j.jmatprotec.2018.04.049
5. Kim, D. M., Bajpai, V., Kim, B. H., & Park, H. W. (2015). Finite element modeling of hard turning process via a micro-textured tool. *The International Journal of Advanced Manufacturing Technology, 78*(9), 1393–1405. https://doi.org/10.1007/s00170-014-6747-x
6. Kawasegi, N., Ozaki, K., Morita, N., Nishimura, K., & Yamaguchi, M. (2017). Development and machining performance of a textured diamond cutting tool fabricated with a focused ion beam and heat treatment. *Precision Engineering, 47*, 311–320. https://doi.org/10.1016/j.precisioneng.2016.09.005
7. Kang, Z., Fu, Y., Chen, Y., Ji, J., Fu, H., Wang, S., & Li, R. (2018). Experimental investigation of concave and convex micro-textures for improving anti-adhesion property of cutting tool in dry finish cutting. *International Journal of Precision Engineering and Manufacturing-Green Technology, 5*(5), 583–591. https://doi.org/10.1007/s40684-018-0060-3
8. Lian, Y., Chen, H., & Mu, C. (2019). Performance of micro-textured tools fabricated by inductively coupled plasma etching in dry cutting tests on medium carbon steel workpieces. *International Journal of Precision Engineering and Manufacturing-Green Technology, 6*(2), 175–188. https://doi.org/10.1007/s40684-019-00088-3
9. Zhang, K., Guo, X., Wang, C., Meng, X., Sun, L., & Xing, Y. (2020). Effect of scale and sequence of surface textures on the anti-adhesive wear performance of PVD coated tool in dry machining SLM-produced stainless steel. *International Journal of Precision Engineering and Manufacturing-Green Technology*. https://doi.org/10.1007/s40684-020-00233-3
10. Maeng, S., & Min, S. (2020). Dry ultra-precision machining of tungsten carbide with patterned nano PCD tool. *Procedia Manufacturing, 48*, 452–456. https://doi.org/10.1016/j.promfg.2020.05.068
11. Shamoto, E., & Moriwaki, T. (1994). Study on elliptical vibration cutting. *CIRP Annals, 43*(1), 35–38. https://doi.org/10.1016/S0007-8506(07)62158-1
12. Shamoto, E., & Moriwaki, T. (1999). Ultaprecision diamond cutting of hardened steel by applying elliptical vibration cutting. *CIRP Annals, 48*(1), 441–444. https://doi.org/10.1016/S0007-8506(07)63222-3
13. Kim, G. D., & Loh, B. G. (2011). Direct machining of micro patterns on nickel alloy and mold steel by vibration assisted cutting. *International Journal of Precision Engineering and Manufacturing, 12*(4), 583–588. https://doi.org/10.1007/s12541-011-0075-y
14. Liu, K., Li, X. P., Rahman, M., & Liu, X. D. (2004). Study of ductile mode cutting in grooving of tungsten carbide with and without ultrasonic vibration assistance. *The International Journal of Advanced Manufacturing Technology, 24*(5), 389–394. https://doi.org/10.1007/s00170-003-1647-5
15. Suzuki, N., Haritani, M., Yang, J., Hino, R., & Shamoto, E. (2007). Elliptical vibration cutting of tungsten alloy molds for optical glass parts. *CIRP Annals, 56*(1), 127–130. https://doi.org/10.1016/j.cirp.2007.05.032
16. Brehl, D. E., & Dow, T. A. (2008). Review of vibration-assisted machining. *Precision Engineering, 32*(3), 153–172. https://doi.org/10.1016/j.precisioneng.2007.08.003
17. Jung, H., Hayasaka, T., & Shamoto, E. (2018). Study on process monitoring of elliptical vibration cutting by utilizing internal data in ultrasonic elliptical vibration device. *International Journal of Precision Engineering and Manufacturing-Green Technology, 5*(5), 571–581. https://doi.org/10.1007/s40684-018-0059-9
18. Jiang, C., Wu, T., Ye, H., Cheng, J., & Hao, Y. (2019). Estimation of energy and time savings in optical glass manufacturing when using ultrasonic vibration-assisted grinding. *International Journal of Precision Engineering and Manufacturing-Green Technology, 6*(1), 1–9. https://doi.org/10.1007/s40684-019-00022-7
19. Zhang, J., Rosenkranz, A., Zhang, J., Guo, J., Li, X., Chen, X., Xiao, J., & Xu, J. (2021). Modified wettability of micro-structured steel surfaces fabricated by elliptical vibration diamond cutting. *International Journal of Precision Engineering and Manufacturing-Green Technology*. https://doi.org/10.1007/s40684-021-00358-z
20. Shimada, S., Tanaka, H., Higuchi, M., Yamaguchi, T., Honda, S., & Obata, K. (2004). Thermochemical wear mechanisms in machining of ferrous metals. *CIRP Annals, 53*(1), 57–60. https://doi.org/10.1016/S0007-8506(07)60644-1

Sangjin Maeng is an assistant professor at Mechanical and System Design Engineering, Hongik University. He has worked at Samsung SDI in 2012 where his team developed a winder machine for lithium-ion batteries. He is currently working on the ultra-precision machining, geometric error identification, precise tool setting, and smart manufacturing.

Hiroaki Ito is a master course student at School of Integrated Design Engineering, Graduate School of Science and Technology, Keio University. He is currently working on the elliptical vibration assisted cutting with textured tools.

Yasuhiro Kakinuma is full professor at Department of System Design Engineering, Keio University. He is currently working on three major topics: UPM (Ultra-Precision Machining), Observer-based Process Monitoring and Control, and Metal Additive Manufacturing.

Sangkee Min is associate professor at Department of Mechanical Engineering, University of Wisconsin-Madison. He is currently working on three major research topics: UPM (Ultra-Precision Machining), SSM (Smart Sustainable Manufacturing), and MFD (Manufacturing for Design).